

Intelligent Control for Self-erecting Inverted Pendulum Via Adaptive Neuro-fuzzy Inference System

¹A.A. Saifizul, ¹Z. Zainon, ²N.A Abu Osman, ³C.A. Azlan and ⁴U.F.S Ungku Ibrahim

¹Department of Mechanical Engineering, Faculty of Engineering
University of Malaya, 50603, Kuala Lumpur, Malaysia

²Department of BioMedical Engineering, Faculty of Engineering
University of Malaya, 50603, Kuala Lumpur, Malaysia

³Department of BioMedical-Imaging, Faculty of Medicine
University of Malaya, 50603, Kuala Lumpur, Malaysia

⁴Center for Foundation Studies in Science, University of Malaya
50603 Kuala Lumpur, Malaysia

Abstract: A self-erecting single inverted pendulum (SESIP) is one of typical nonlinear systems. The control scheme running the SESIP consists of two main control loops. Namely, these control loops are swing-up controller and stabilization controller. A swing-up controller of an inverted pendulum system must actuate the pendulum from the stable position. While a stabilization controller must stand the pendulum in the unstable position. To deal with this system, a lot of control techniques have been used on the basis of linearized or nonlinear model. In real-time implementation, a real inverted pendulum system has state constraints and limited amplitude of input. These problems make it difficult to design a swing-up and a stabilization controller. In this paper, first, the mathematical models of cart and single inverted pendulum system are presented. Then, the Position-Velocity controller is designed to swing-up the pendulum considering physical behavior. For stabilizing the inverted pendulum, a Takagi-Sugeno fuzzy controller with Adaptive Neuro-Fuzzy Inference System (ANFIS) architecture is used to guarantee stability at unstable equilibrium position. Experimental results are given to show the effectiveness of these controllers.

Key words: Takagi-sugeno fuzzy, ANFIS, self-erecting inverted pendulum

INTRODUCTION

The self-erecting single inverted pendulum (SESIP) system is a challenging problem in the area of control systems. It is very useful to demonstrate concepts in linear control such as the stabilization of unstable systems. Besides, as a typical unstable non-linear system, inverted pendulum system is often used as a benchmark for verifying the performance and effectiveness of a new control method because of the simplicities of the structure.

The control strategy of SESIP system is composed of the swing-up control of the pendulum and the stabilizing control of the whole system that consists of angular control of the pendulum at upright position and position control of the cart at origin of rail. First, swing-up control is to bring the pendulum from the downwards position to the upright position. This is achieved when the motor is given voltage in the appropriate direction and magnitude to drive the cart back and forth along the extremely limited track length repeatedly until the pendulum is close to the upright position. Thereafter, stabilizing control is to balance the

pendulum in the upright position. When the pendulum leans in one direction, the control algorithm will try to move the cart under it with appropriate speed and direction. In this case, the algorithm will take the inputs i.e. the pendulum angle and cart position measured by encoders, then tell the cart which way and how fast to move.

Until now, a lot of intelligent approaches about the swing-up and stabilizing control of inverted pendulum system have been proposed. Mikukcic and Chen^[1] extracted fuzzy rules for inverted pendulum control by fuzzy clustering method. Brock^[2] has presented the fuzzy PD controller in balancing the pendulum in upright position and then the tuning process is done using evolutionary algorithms. He has successfully proved the robustness of the controller in simulated experiment. Kandadai and Tien^[3] presented neuro-fuzzy architecture to automatically generate a fuzzy knowledge based by a pseudo-supervised learning scheme. It takes more than 12 s and its structure is more complex. Kawaji and Maeda^[4] constructed a simple fuzzy controller that impeded the position control of the cart as a virtual target angle into the angular control of

the pendulum, but the controller was difficult to completely stabilize a pendulum system within a short time.

Since most of the classical fuzzy approach will cause the exponential increase in complexity, Horikawa *et al.*^[5], Lin and Lee^[6], Partricar and Provence^[7] and Takagi and Hayashi^[8] presented techniques incorporating neural network into Fuzzy system. Kyung and Lee^[9] presented a fuzzy controller, whose rule base was derived from three neural networks. Although the fuzzy controller can stabilize an inverted pendulum system in about 8.0 s, it needs 396 rules. Sakai and Takahama^[10] applied a nonlinear optimization method to train a fuzzy controller for stabilization. However, the controller spent more than 200.0 s on stabilizing an inverted pendulum system.

In this paper, a position-velocity (PV) is used for swing-up control while a data-driven Takagi-Sugeno Fuzzy model called ANFIS is employed for the stabilizing control. A common Takagi-Sugeno fuzzy model approach typically uses common sense knowledge of human experts which tends to be “trial and error” in tuning its membership functions and rules. It may be less suitable for control design. Therefore, the ANFIS controller which was developed by^[11] is used to solve the SESIP stabilizing problem. This method is proposed to construct the fuzzy model by combining information obtained from measured data i.e. training data and checking data with heuristic knowledge expressed in the form of rules. Initially, the expert knowledge is formulated as a collection of if-then rules and the associated membership functions. But then, these rules and membership functions can be fine-tuned by using numerical data. This model tends to be adaptive. It is able to adjust itself to accommodate new situation, especially changes in the dynamic behavior of the SESIP plant in order to achieve the desired performance objective.

Modeling of cart system: The cart system can be represented as follows:

$$G(s) = \frac{x_c(s)}{V_m(s)} \quad (1)$$

where $G(s)$ is open-loop transfer function, x_c is cart position and V_m is motor voltage. Applying Newton's second law of motion to the cart system and by assuming cart's Coulumb friction is neglected, the equation of motion can be represented as follows:

$$M \ddot{x}_c(t) = F_c(t) - B_{eq} \dot{x}_c(t) - F_{ai}(t) \quad (2)$$

where F_c is cart driving force produced by the motor and F_{ai} is inertial force due to the motor's armature in rotation and other parameters are given in Table 1. The driving force, F_c , generated by the DC motor and

Table 1: List of symbols and model parameters

acting on the cart through the motor pinion can be expressed as:

$$F_c(t) = \frac{\eta_g K_g T_m(t)}{r_{mp}} \quad (3)$$

where T_m is torque generated by the motor.

Using Kirchhoff's Voltage law, the following equation is obtained:

$$V_m(t) - R_m I_m(t) - L_m \left(\frac{\partial}{\partial t} I_m(t) \right) - E_{emf}(t) = 0 \quad (4)$$

However, since $L_m \ll R_m$, the motor inductance is disregarded and yields:

$$I_m(t) = \frac{V_m(t) - E_{emf}(t)}{R_m} \quad (5)$$

Since the back-emf voltage created by the motor, E_{emf} , is proportional to the motor shaft velocity w_m , the equation is obtained as:

$$I_m(t) = \frac{V_m(t) - K_m w_m(t)}{R_m} \quad (6)$$

Moreover, in order to account for the DC motor electrical losses, the motor efficiency is introduced to calculate the torque generated by the DC motor:

$$T_m(t) = \eta_m K_t I_m(t) \quad (7)$$

Substituting (6) and (7) into (3) leads to:

$$F_c(t) = \frac{\eta_g K_g \eta_m K_t (V_m(t) - K_m w_m(t))}{R_m r_{mp}} \quad (8)$$

By considering the rack and pinion and the gearbox mechanisms, the motor angular velocity can be written as a function of the cart linear velocity, as expressed by:

$$w_m(t) = \frac{K_g \dot{x}(t)}{r_{mp}} \quad (9)$$

Therefore, substituting (9) into (8) and rearranging leads to:

$$F_c(t) = \frac{\eta_g K_g \eta_m K_t (r_{mp} V_m(t) - K_g K_m \dot{x}(t))}{R_m r_{mp}^2} \quad (10)$$

As seen at the motor pinion, the armature inertial force due to the motor rotation and acting on the cart can be expressed as a function of the armature inertial torque:

$$F_{ai} = \frac{\eta_g K_g T_{ai}}{r_{mp}} \quad (11)$$

Applying Newton's second law of motion to the motor shaft:

$$J_m \ddot{\theta}_m(t) = T_{ai}(t) \quad (12)$$

where θ_m is motor shaft rotation angle. Moreover, the mechanical configuration of the cart's rack-pinion system gives the following relationship:

Symbol	Description	Value/Unit
V_m	Motor nominal input voltage	6 V
R_m	Motor armature resistance	2.6 Ω
L_m	Motor armature inductance	0.18 mH
K_t	Motor torque constant	0.00767 Nm/A
η_m	Motor efficiency	100%
K_m	EMF constant	0.00767 Vs/rad
J_m	Rotor moment inertia	3.9×10^{-7} kgm ²
K_g	Planetary gearbox gear ratio	3.71
η_g	Planetary gearbox efficiency	100%
r_{mp}	Motor pinion radius	6.35×10^{-3} m
r_{pp}	Position pinion radius	1.48×10^{-2} m
B_{eq}	Equivalent viscous damping coefficient at the motor pinion	5.4 Nms/rad
B_p	Viscous damping coefficient at the pendulum pivot	0.0024 Nms/rad
l_p	Pendulum length length from pivot to center of gravity	0.3302 m
I_p	Pendulum moment of inertia	7.88×10^{-3} kg m ²
M_p	Pendulum mass	0.230 kg
M	Cart mass	0.94 kg

$$\theta_m = \frac{K_g x}{r_{mp}} \quad (13)$$

Substituting (11) and (12) into (10)

$$F_{ai} = \frac{\eta_g K_g^2 J_m \ddot{x}(t)}{r_{mp}^2} \quad (14)$$

Finally, substituting (10) and (14) into (2), applying the Laplace transform and rearranging, yields the desired open loop transfer function for the cart system, such that:

$$G(s) = \frac{r_{mp} \eta_g K_g \eta_m K_t}{((R_m M r_{mp}^2 + R_m \eta_g K_g^2 J_m) s + \eta_g K_g^2 \eta_m K_t K_m + B_{eq} R_m r_{mp}^2) s} \quad (15)$$

Single inverted pendulum equation of motion: Angle definitions and schematic diagram of SESIP are shown in Fig. 1.

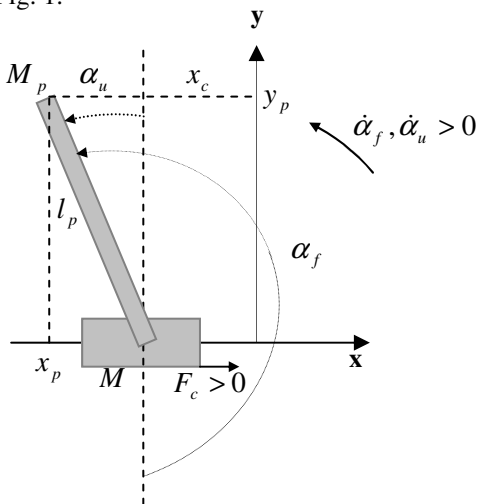


Fig. 1: SESIP schematic

The SIP system system is made of a cart on top of which pendulum is pivoted. The cart is constrained to move only in the horizontal x direction, while the pendulum can only rotate in the x - y plane. The SIP system has two degrees of freedom and can therefore be

fully represented using two generalized coordinates: Horizontal displacement of the cart, x_c ; and Rotational displacement of pendulum, α . Assume the (nonlinear) Coulomb friction applied to the linear cart is assumed to be neglected. Moreover, the force on the linear cart due to the pendulum's action has also been neglected in the presently developed model. A nonlinear equation of motion (OEM) of single inverted pendulum (SIP) system can be derived using Lagrange's equation.

$$\frac{d}{dt} \left[\frac{\partial L}{\partial \dot{x}_c} \right] - \frac{\partial L}{\partial x_c} = Q_{x_c} \quad (16)$$

and

$$\frac{d}{dt} \left[\frac{\partial L}{\partial \dot{\alpha}} \right] - \frac{\partial L}{\partial \alpha} = Q_{\alpha} \quad (17)$$

with $L = T_T - V_T$ where T_T is total kinetic energy, V_T is total potential energy, Q_{x_c} and Q_{α} are the generalized force applied on the generalized coordinate x_c and α , respectively. Both generalized forces can be defined as below:

$$Q_{x_c}(t) = F_c(t) - B_{eq} \dot{x}_c \quad (18)$$

and

$$Q_{\alpha}(t) = -B_p \dot{\alpha}(t) \quad (19)$$

This energy is usually caused by its vertical displacement from normality (gravitational potential energy) or by a spring-related sort of displacement (elastic potential energy). In this case; there is no elastic potential energy in the system. The system potential energy is only due to gravity. The cart linear motion is horizontal and as such, never has vertical displacement. Therefore, the total potential energy is fully expressed by the pendulum's gravitational potential energy, as characterized below:

$$V_T = M_p g l_p \cos(\alpha(t)) \quad (20)$$

The kinetic energy measures the amount of energy in a system due to its motion. Here, the total kinetic energy can be represented as follows:

$$T_T = T_c + T_p \tag{21}$$

where T_c and T_p are the sum of the translational and rotational kinetic energies arising from both the cart and its mounted inverted pendulum, respectively. First, the translational kinetic energy of the motorized cart, T_{ct} , is expressed as follows:

$$T_{ct} = \frac{1}{2} M \dot{x}_c^2 \tag{22}$$

Second, the rotational kinetic energy due to the cart's DC motor, T_{cr} , can be characterized by:

$$T_{cr} = \frac{1}{2} \frac{J_m K_g^2 \dot{x}_c^2}{r_{mp}^2} \tag{23}$$

Therefore, the cart's total kinetic energy, can be written as shown below:

$$T_c = \frac{1}{2} M_c \dot{x}_c^2 \tag{24}$$

where $M_c = M + (J_m K_g^2 / r_{mp}^2)$.

The pendulum total kinetic energy, T_p is combined of translational kinetic energy, T_{pt} and rotational kinetic energy, T_{pr} .

$$T_p = T_{pt} + T_{pr} = \frac{1}{2} M_p \dot{x}_p^2 + \frac{1}{2} I_p \dot{\alpha}^2(t) \tag{25}$$

where $\dot{x}_p^2 = \dot{x}_c^2 + \dot{y}_p^2$. From Fig. 2, \dot{x}_p and \dot{y}_p can be expressed as:

$$\dot{x}_p = \dot{x}_c - l_p \cos(\alpha(t)) \dot{\alpha}(t) \tag{26}$$

and

$$\dot{y}_p = -l_p \sin(\alpha(t)) \dot{\alpha}(t) \tag{27}$$

Substituting (24), (25), (26), (27) into (21), gives the total kinetic energy, T_T of the system as:

$$T_T = \frac{1}{2} (M_c + M_p) \dot{x}_c^2 - M_p l_p \cos(\alpha(t)) \dot{\alpha}(t) \dot{x}_c(t) + \frac{1}{2} (I_p + M_p l_p^2) \dot{\alpha}^2(t) \tag{28}$$

The Lagrangian can be expressed using (20) and (28):

$$L = T_T - V_T = \frac{1}{2} (M_c + M_p) \dot{x}_c^2(t) - M_p l_p \cos(\alpha(t)) \dot{\alpha}(t) \dot{x}_c(t) + \frac{1}{2} (I_p + M_p l_p^2) \dot{\alpha}^2(t) - M_p l_p \cos(\alpha(t)) \tag{29}$$

From equation (16) and (17), the nonlinear equation of motion can be obtained as:

$$(M_c + M_p) \ddot{x}_c(t) + B_{eq} \dot{x}_c(t) - (M_p l_p \cos(\alpha(t))) \ddot{\alpha}(t) + M_p l_p \sin(\alpha(t)) \dot{\alpha}^2(t) = F_c(t) \tag{30}$$

and

$$-M_p l_p \cos(\alpha(t)) \ddot{x}_c(t) + (I_p + M_p l_p^2) \ddot{\alpha}(t) + B_p \dot{\alpha}(t) - M_p g l_p \sin(\alpha(t)) = 0 \tag{31}$$

The linearized model of (30) and (31) can be obtained by considering the small variations of α about the equilibrium point when the pendulum is at upright position and neglecting higher order term. The linearized model can be expressed in state space representation as follows:

$$\dot{\mathbf{x}} = A \mathbf{x} + B \mathbf{u} \tag{32}$$

$$y = C \mathbf{x}$$

where, $\mathbf{x} = [x_c \ \alpha \ \dot{x}_c \ \dot{\alpha}]^T$, $\mathbf{u} = F_c$ and

$y = [x_c \ \alpha]^T$ and matrix A , B and C are given as:

$$A = \begin{bmatrix} 0 & 0 & 1 & 0 \\ 0 & 0 & 0 & 1 \\ 0 & \frac{(M_p l_p)^2 g}{Z} & -\frac{B_{eq}(M_p l_p^2 + I)}{Z} & -\frac{M_p l_p B_p}{Z} \\ 0 & \frac{(M_p + M_c) M_p g l_p}{Z} & -\frac{M_p l_p B_{eq}}{Z} & -\frac{(M_p + M_c) B_p}{Z} \end{bmatrix}$$

$$B = \begin{bmatrix} 0 \\ 0 \\ \frac{Z}{(I + M_p l_p^2)} \\ \frac{M_p l_p}{Z} \end{bmatrix} \quad C = \begin{bmatrix} 1 & 0 & 0 & 0 \\ 0 & 1 & 0 & 0 \end{bmatrix}$$

where $Z = (M_c + M_p) I_p + M_c M_p l_p^2$

SESIP control strategy model: The control strategy to implement the SESIP consists of two main control loops and a decision-making logic component to switch between the two. One control loop is a PV controller on the cart position in order to swing up the single pendulum from the suspended to the inverted posture. The other control loop is active when the pendulum is around the upright position and consists of maintaining the inverted pendulum vertical. It uses a TS fuzzy controller with ANFIS architecture.

Swing-up controller design: To control the cart, a control strategy based on the proportional-velocity (PV) control scheme is used in order to to make the closed-loop system to satisfy the following performance requirements:

- * The percent overshoot (PO) should be less than 10% i.e. PO<10%
- * The time to first peak should be 150ms i.e. $t_p = 0.15$ s.

The PV control law can be expressed as follows:

$$V_m(t) = K_p (x_d(t) - x_c(t)) - K_v \dot{x}_c(t) \tag{33}$$

where x_d is the reference signal i.e. the desired position to track. Then, the closed-loop transfer function can be expressed as:

$$\frac{x_c(s)}{x_d(s)} = \frac{K_p G(s)}{1 + K_p G(s) + G(s)K_v s} \quad (34)$$

Replacing $G(s)$ in equation (15) into (34) and using model parameter values in Table 1 leads to the following:

$$\frac{x_c(s)}{x_d(s)} = \frac{2.46K_p}{s^2 + (2.46K_v + 17.13)s + 2.46K_p} \quad (35)$$

According to performance requirements, $PO=10\%$ and $t_p = 0.15s$, a natural frequency, $\omega_n = 26.0 \text{ rad/s}$ and damping ratio, $\zeta = 0.59$ can be obtained. The characteristic equation of the closed-loop transfer function expressed in its standard form is as follows:

$$s^2 + 2\zeta\omega_n s + \omega_n^2 \quad (36)$$

Comparing (35) and (36) lead to the following PV controller gains:

$$K_p = 274.62 \text{ V/m and } K_v = 5.53 \text{ Vs/m.}$$

Stabilizing controller design: Based on (32), the Takagi-Sugeno (TS) fuzzy controller develop here has four inputs i.e. x_c , α , \dot{x}_c and $\dot{\alpha}$ and a single output i.e. V_m . These four input variables considerably affect the control action, V_m which is applied to the cart motor. The control problem here is to design a controller that maps the state vector x into an appropriate control action, V_m , such that the pendulum is kept balanced while the cart is tracking back to its origin of track. In addition, the choice of membership functions (MFs) and rule base of the TS fuzzy controller will affect the performance of the system. The TS fuzzy controller with ANFIS architecture can formalize a systematic approach to generate the fuzzy rule and MFs.

Training data set: The training data set that contains the desired input/output data pairs of the actual plant is obtained through the real-time experiments. Figure 2 and 3 show block diagram of real-time implementation for collecting input-output data pairs of the inverted pendulum which is in the following format:

$$\left[\underbrace{x_c, \alpha, \dot{x}_c, \dot{\alpha}}_{\text{input variables}} \quad \underbrace{V_m}_{\text{output variable}} \right]$$

Also from the experiment, we manage to get 100 sets of checking data of similar format as above.

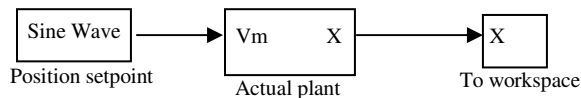


Fig. 2: Block diagram of real-time implementation

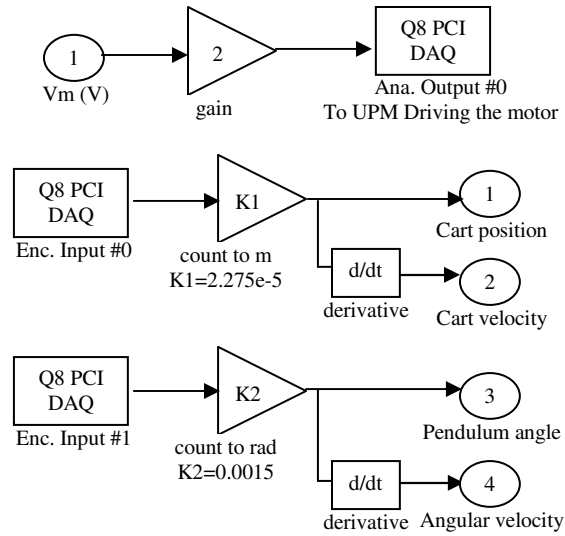


Fig. 3: Actual plant subsystem

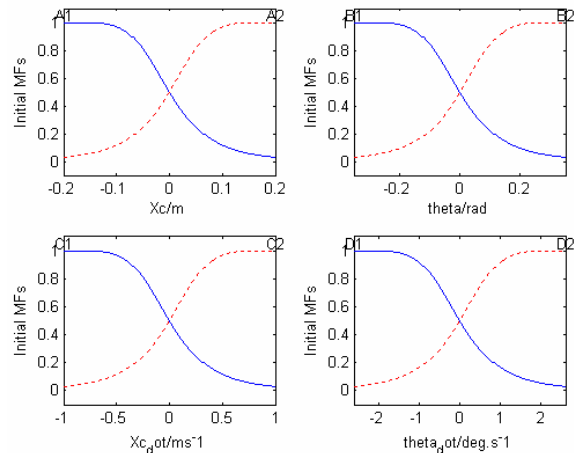


Fig. 4: Initial membership functions for fuzzy controller

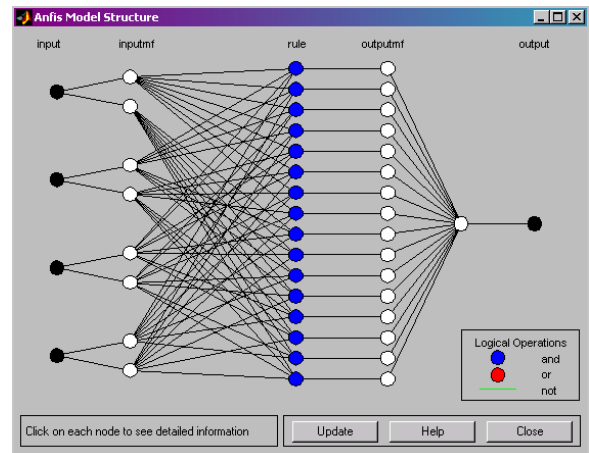


Fig. 5: ANFIS model structure

Initial TS fuzzy inference system: The initial linear relationship between input and output are described in

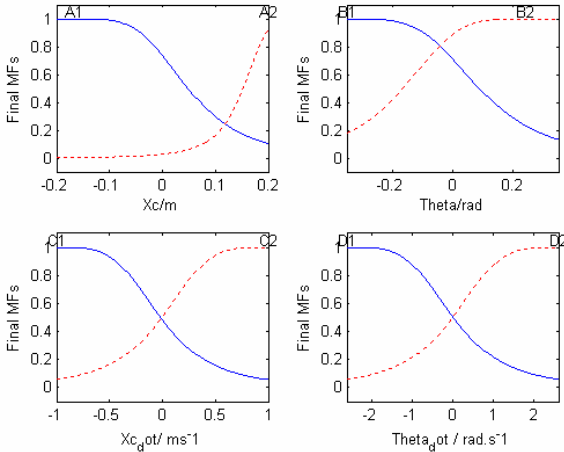


Fig. 6: Final membership functions for ANFIS controller

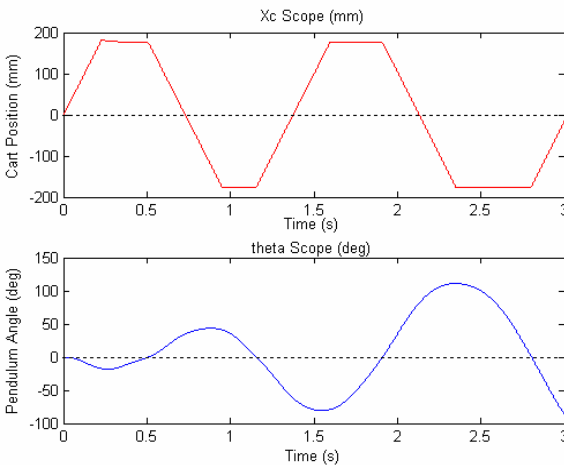


Fig. 7: Simulation results for swing-up control

16 fuzzy-if-then rules which are represented in the format as:

Rule i : IF (x_c is A_j) and (α is B_j) and (\dot{x}_c is C_j) and ($\dot{\alpha}$ is D_j),

$$\text{THEN } (V_m = p_i x_c + q_i \alpha + r_i \dot{x}_c + s_i \dot{\alpha} + t_i) \quad (37)$$

where $i = 1, 2, \dots, 16; j = 1, 2$.

The input MFs for initial fuzzy inference system (FIS) in (37) is shown in Fig. 4.

Trained TS fuzzy inference system: Figure 5 shows ANFIS model structure using ANFIS GUI editor from MathWork Inc. During the training process, the hybrid method with the combination of backpropagation and least square method is implemented to estimate MFs parameters.

Finally, a trained FIS structure is created from the initial FIS using ANFIS GUI editor and training and checking data sets. The MFs of trained FIS are shown in Fig. 6. The output parameters and rule base of trained data cannot be shown here due to limited space.

Simulation

Swing-up control simulation: From Fig. 7, the cart is moving alternately between 180 mm and -180 mm to increase the energy of the system as quickly as possible by moving the cart to its maximum allowed distance of track (i.e. 0.2 m). In this swing-up mode, PV controller destabilizes the pendulum when initially at rest and hanging down. The amplitude of the pendulum angle become larger until it is close to the upright position, so that the stabilizing controller will catch the pendulum and balance it later. As can be seen in the simulation results, the PV controller takes 2.5 s for 4 swings. Thus, the PV controller could be effectively employed in SESIP control system as a swing-up controller to get maximum swing in the shortest possible time.

Stabilizing control simulation: Figures 8 and 9 show control results of the inverted pendulum system by Simulink simulation.

In Fig. 9, the initial angle of the pendulum is 10 degree and the other initial values are all zeros. Since the initial value of the pendulum is positive to the left, the cart is first driven from the original position to the left side (which is defined as negative) such that the pendulum rotates clockwise towards upright position. After the pendulum reaches the upright position, it still rotates to the negative (to the right) direction because of its inertia energy of movement. Then the negative driven force moves the cart back towards the origin, causing the pendulum to stand up eventually. It takes 2.75 s to be stabilized. In Fig. 10, the cart is applied an input of square-wave signal with 20 mm of amplitude. The signal frequency is set to 0.1 Hz. The pendulum system is managed to be stabilized in upright position, even though the disturbance is applied to the cart position alternately. In this case, the robustness of the SESIP system is successfully realized by the proposed ANFIS controller.

RESULTS

Real-time experiment configuration consists of computer with MATLAB, Simulink and Quanser Toolbox used as a controller, Q8 data acquisition board and Quanser IP02 Linear Motion Servo Module. Some hardware limitations should be concerned in the cart-pendulum system. The Digital-to-Analog voltage for data acquisition board is limited between -10 V and 10 V. The safety watchdog is turned on where the allowable cart displacement is 0.35 m from the centre of the track. When the pendulum or cart touches the limit switch, the control process is aborted. Figures 11 to 13 show the SESIP control system experimental results.

It is important to note that the PV controller takes approximately 3.5 seconds to reach the upright position. The point at which the ANFIS controller catches the pendulum in the upright position is clearly shown in the above plots.

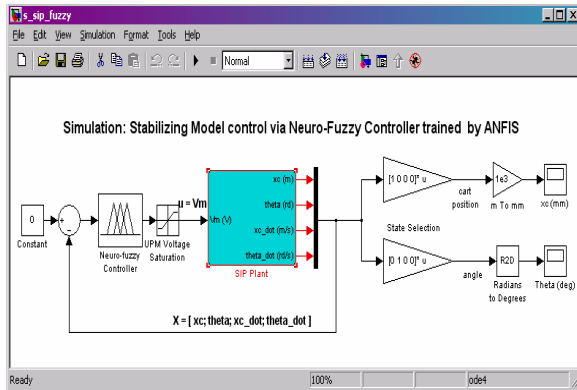


Fig. 8: Simulink diagram of balance control

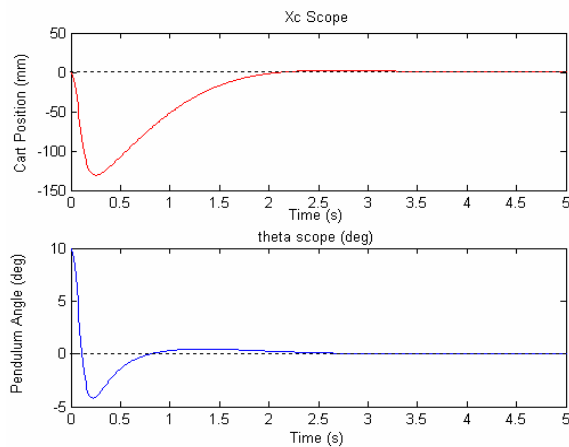


Fig. 9: Simulation results for stabilization control

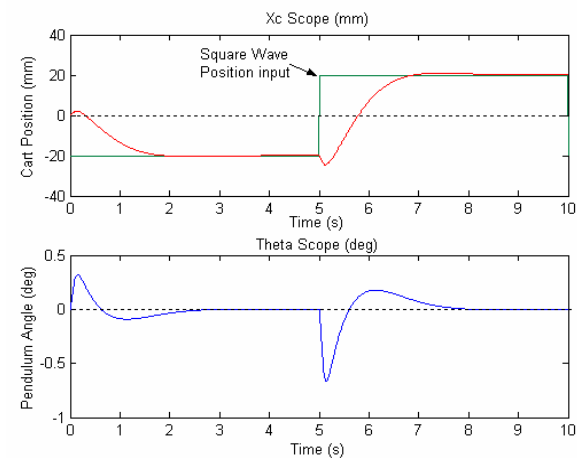


Fig. 10: Simulation results for stabilization control when system is applied square-wave position input

Figure 11 shows that the control output, V_m for control of SESIP system is not constant all the way. Initially maximum V_m that is 10 V (in our experiment, the voltage saturation is limited to be 10 V) supplied to the cart motor in its attempt to start the pendulum from rest. Then the voltage decreases a bit when the pendulum is falling naturally by the gravitational

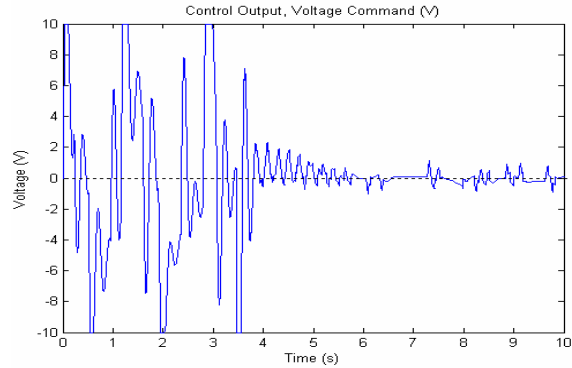


Fig. 11: Voltage output for cart motor

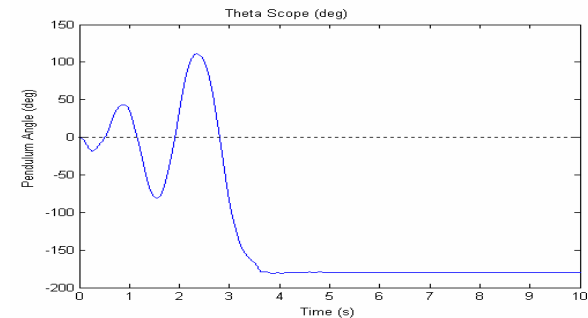


Fig. 12: Experimental result of pendulum angle, θ

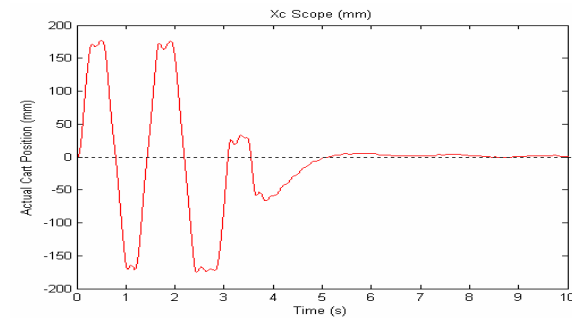


Fig. 13: Experimental result of cart position, x_c

potential energy. To regain energy to swing up the pendulum, the maximum voltage is supplied to the cart again. This phenomenon continues until the pendulum reaches within 15 degree from the upright position. The trend of voltage command explained above is fed by PV controller of swing-up mode. Once the stabilizing controller is activated and catches the pendulum, the output voltage starts to decrease greatly in magnitude because less energy is needed to control the small deviation of pendulum in balance mode. In this case, the voltage supplied is in the range of ± 1 V which is controlled by ANFIS controller. The corresponding plot of the pendulum angle is shown in Fig. 12. Each swing increases the pendulum angle slightly until the pendulum is closed to the upright position, which is defined to be 180 degree from its initial hanging down position. At that stage, the pendulum angle remains fairly constant. Note that the controller takes about 4 swings to bring the pendulum close enough to upright

position within 3.5 s. After that, it remains stabilized throughout the experimental period for no matter how long it is. It is indicated that the switch is triggered effectively so that the ANFIS controller could catch the pendulum and balance it completely. Figure 13 depicts the cart linear position for the entire control process. Initially, the cart linear displacement alternates between 180 mm and -180 mm.

As can be seen, a few cart large movements are done, until about 3 s, the pendulum amplitude of oscillation becomes large enough to be beyond 150 degree from the downward position. Then, it takes the smaller cart position set point amplitude about another 0.5 s to slowly bring the pendulum close to the upright position. Once the pendulum is almost balanced, the cart will return to its origin of track within 1.5 s, which is at 5 s of the experimental time. Slight errors appear at the maximum displacement of the cart because this is the time when the cart abruptly changes its direction.

Consequently, as can be seen from Fig. 12 and 14, the control force optimized by PV controller is able to move the cart back and forth with a minimum number of times and finally bring the pendulum up as quickly (and smoothly) as possible. The stabilization control of the pendulum is also successfully realized in real time by the proposed ANFIS controller.

CONCLUSION

The objective of this project was to design a stabilizing controller for SESIP problem and this has been successfully achieved. The simulation and experimental results show that the hybrid controllers take about 3.5 s and 4 swings to bring the pendulum close to upright position while the stabilizing controller with only 16 fuzzy rules is able to balance the pendulum for the rest of the experiment period. It is worth to note that the cart is able to return to the origin of the rail after the pendulum is stabilized. This controller is proved to be effective and feasible in both of the angular control of pendulum at upright position and position control of cart to its origin of rail.

REFERENCES

1. Mikulcic, A. and J. Chen, 1996. Experiments on using fuzzy clustering for fuzzy control system design. Proc. FUZZ-IEEE'96, 3: 2168-74.
2. Brock, S., 2003. Practical approach to fuzzy control of inverter pendulum. IEEE Intl. Conf. Industrial Technology'03, 1: 31-35.
3. Kandadai, R.M. and J.M. Tien, 1996. On a fuzzy-neural hierarchical controller with a self-generating knowledge base. Proc. IEEE Intl. Conf. on Systems, Man and Cybernetics, 4: 2625-2630.
4. Kawaji, S. and T. Maeda, 1991. Fuzzy servo control system for an inverted pendulum. Proc. Internet Fuzzy Engineering Symp., 2: 812-823.
5. Horikawa, S.I., T. Furuhashi and Y. Uchikawa, 1992. On fuzzy modeling using neural networks with the back propagation algorithm. IEEE Trans. Neural Networks, 3: 801-806.
6. Lin, C.T. and C.S.G. Lee, 1992. Neural network based fuzzy logic control and decision systems. IEEE Trans. Computers, 40: 1320-1336.
7. Patricar, A. and J. Provence, 1990. A self-organizing controller for dynamic processes using neural networks. Intl. Joint Conf. Neural Networks, 3: 359-364.
8. Takagi, H. and I. Hayashi, 1991. NN-driven fuzzy reasoning. Intl. J. Approximate Reasoning, 5: 191-212.
9. Kyung, K.H. and B.H. Lee, 1993. Fuzzy rule base derivation using neural network based fuzzy logic controller by self-learning. Proc. IECON'93, 1: 435-440.
10. Sakai, S. and T. Takahama, 1997. Learning fuzzy control rules for inverted pendulum by simplex method. Proc. of the 13th Fuzzy System Symposium, pp: 61-64.
11. Jang, J.S., 1993. ANFIS: Adaptive-network-based fuzzy inference system. IEEE Trans. Systems, Man and Cybernetics, 23: 665-685.